Polymer Degradation and Stability 119 (2015) 190–197

Contents lists available at ScienceDirect

Polymer Degradation and Stability

journal homepage: www.elsevier.com/locate/polydegstab

Influence of borate structure on the thermal stability of boron-containing phenolic resins: A DFT study

Cheng Bian, Yong Wang, Shujuan Wang, Yuhu Zhong, Yun Liu, Xinli Jing*

Department of Applied Chemistry, School of Science, Xi'an Jiaotong University, Xi'an 710049, China

ARTICLE INFO

Article history:
Received 30 January 2015
Received in revised form
14 April 2015
Accepted 11 May 2015
Available online 20 May 2015

Keywords:
Phenolic resin
Density functional theory
Borate structure
Thermal stability
Bond dissociation energy

ABSTRACT

In the present study, the density functional theory (DFT) was applied to investigate the influence of borate structure on the thermal stability of phenolic resin modified by boric acid (BPR) and phenylboronic acid (PBPR). The bond dissociation energy (BDE) and electronic structure, which represent the stability of chemical bonds and reactivity of functional groups respectively, were obtained with the BPW91, B3LYP, CAM-B3LYP and M06-2X method based on simplified models of BPR and PBPR. The BDE of B—O bond was higher than C—O and C—C bonds, which may contribute to the thermal stability of the resins. Moreover, the population analysis indicated that the formed borate structures from boric hydroxyls and phenolic hydroxyls could inhibit the active sites, such as phenolic hydroxyls and methylenes in PR. The inhibiting effect worked well in both BPR and PBPR, especially in the structures with eight-membered heterocycles formed by the borate and methylene bridges. These results provide useful clues for understanding the roles of borate structure in improving the thermal stability of PR, which are of practical importance in the design and optimization of thermal stable resins.

1. Introduction

The thermal stability of a polymer is limited by the dissociation of weak bonds and the reactivity of the main functional groups. In order to obtain polymer with high thermal stability, chemical bond with high bond dissociation energy (BDE) and functional group with low reactivity are usually needed. Because of its high thermal stability and low-cost, phenolic resin (PR) is widely used for the preparation of thermal protection materials and ablative materials. Some researchers [1,2] pointed out that the pyrolysis of PR at the initial stage contained the homolytic reaction resulting in the formation of free radicals (H·, HO· and Ph·, etc), as well as the reaction between these radicals and the functional groups in the unpyrolyzed zone. The phenolic hydroxyls and methylenes are the active sites in PR because of the low BDEs of O—H, C—O and C—H bonds [3,4]. Therefore, in order to understand the relationship between the cured structure and thermal stability of PR, we should focus on the BDE of the weak bonds in the resin and the reactivity of phenolic hydroxyls, phenol rings and methylenes.

That the introduction of boric acid (BA) or phenylboronic acid (PBA) into PR could obviously improve the thermal stability of PR is largely attributed to the borate structure formed through the reaction of boric hydroxyls and phenolic hydroxyls. Some researchers tended to believe that the BDE of B—O bond in borate structure was higher than C—C bond in methylene bridge, which could postpone the decomposition of PR [5,6]. Our previous study showed that the effect of borate structure may not be limited to the bond strength of B—O bond, the network of BPR and PBPR was significantly changed in comparison with PR [7,8]. However, the experimental evidence is not sufficient and an analysis based on BDE and electronic structure of the groups linked to the borate structure would be helpful.

Several quantum chemistry methods, usually based on simplified models, have already been used in attempts to calculate the BDE of chemical bond and evaluate the reactivity of functional group in polymer. For instance, Conner et al. [9,10] investigated the reactivity of different phenolic compounds (with formaldehyde) through *ab initio* approach. The results showed that the reactivity of phenolic compounds was correlated with the electrostatic charge at reactive sites in the phenolic ring. Khavryuchenko et al. [11] simulated the pyrolysis process of phosphoric acid modified PR with a semi-empirical method of PM6. Their results showed that the introduction of phosphates dramatically changed the carbonization process of PR. Among the quantum chemistry methods, density functional theory (DFT) has gained immense popularity

* Corresponding author. Tel.: +86 29 68640809.
E-mail address: rgfp-jing@mail.xjtu.edu.cn (X. Jing).

http://dx.doi.org/10.1016/j.polymdegradstab.2015.05.009
0141-3910/

over the past few decades due to its high computational efficiency and accuracy [12]. Based on the simplified graphene-like models of boron modified C/C composites, Wu et al. [13] studied the influence of boron substitution on the reactivity of carbon atoms next to the boron atoms through both DFT and *ab initio* methods. Their results indicated that the BDE of C–C bond calculated on the B3LYP/6-31G(d) level was in excellent agreement with the results on HF/6-31G(d) level. Besides, the HOMO distribution of boron-containing models was also identical.

The above studies showed that based on simplified models of BPR/PBPR and DFT approach, the relationship between borate structure and thermal stability of resins could be further understood. The pristine PR could be represented as PR-1 (Fig. 1) and the positions where the phenol ring crosslinked to the other phenol rings were blocked by methyls. Such model was also adopted by Qi et al. [14] to simulate the initial stage of the pyrolysis of PR. With the attempt to compare the thermal stability of C–C–C bridge (in PR-1) with C–O–B–O–C bridge (in BPR and PBPR), two sets of models containing borate structure can be adopted: i) C–O–B–O–C bridged phenol rings (denoted as BPR-1 and PBPR-1); ii) C–C–C and C–O–B–O–C jointly bridged phenol rings (denoted as BPR-2 and PBPR-2).

The main goal of this work is to obtain the BDEs of the main chemical bonds and the reactivity of the main functional groups in the above models. Meanwhile, we expect to establish an effective method that could be widely used to study the relationship between structure and thermal stability of PR. To achieve these objectives, DFT methods of BPW91, B3LYP, CAM-B3LYP and M06-2X were applied to calculate BDE and bond order of main chemical bonds in the above models, as well as the atomic charges, Fukui function and molecular orbitals. The results of this study will help us to determine whether borate bridged structures could exhibit higher bond strength and lower reactivity, and how could the borate structure affect the thermal stability of the boron-neighbouring structure.

2. Computational details

All the five models were optimized at the BPW91/6-31G*, B3LYP/6-31G*, B3LYP-D3/6-31G* [15–18], CAM-B3LYP/def2-TZVP [19,20] and M06-2X-D3/def2-TZVP [21] levels, with a tolerance of "*verytight*" for the optimization and SCF jobs. Among the four hybrid functionals, CAM-B3LYP (19% HF exchange for short range and 65% for long range) and M06-2X (54% HF exchange) are better than B3LYP (20% HF exchange) in describing the long range interaction, which would benefit BDE calculation. Dispersion correction method DFT-D3, which is a mix of conventional functionals and an add-on energy term, was performed by Grimme's DFT-D3 program package [22]. Owing to its precisely description of the weak interaction, DFT-D3 corrected hybrid functionals achieve CCSD(T) accuracy [22], especially for thermochemical calculation [23]. With good quality and high efficiency, def2-TZVP would be better than 6-31G* in BDE calculation and have already been widely adopted to calculate BDE [24,25]. The vibrational frequencies were calculated at the same level for characterizing the nature of structures and for zero-point energy corrections. All calculations were performed using the Gaussian 09 [26].

Mayer bond order [27], Fukui function [28] and molecular orbital distribution were obtained on BPW91/6-31G*, B3LYP/6-31G*, B3LYP-D3/6-311G**, CAM-B3LYP/6-311G** and M06-2X-D3/6-311G** levels. As the reactivity analysis preferred to be regional, the introduction of diffusion function may lead to unreliable results, thus the triple zeta basis set def2-TZVP was not adopted in this part of calculation. To calculate $f^0(\mathbf{r})$ (Fukui function for free radical attack), the wavefunction of these models with neutral (Q = 0), cationic (Q + 1) and anionic (Q − 1) charges were also obtained.

$$f_N^0(\mathbf{r}) = \frac{1}{2}[\rho_{N+1}(\mathbf{r}) - \rho_{N-1}(\mathbf{r})] \tag{1}$$

$$f_k^0 = \frac{1}{2}[p_k(N+1) - p_k(N-1)] \tag{2}$$

Where $f_N^0(\mathbf{r})$ denotes the Fukui function for free radical attack of a molecular with N electrons, $f_K^0(\mathbf{r})$ denotes the consensed Fukui indice for free radical attack of atom k; $\rho_{N+1}(\mathbf{r})$ and $\rho_{N-1}(\mathbf{r})$ denote electron density of a molecular with N+1 and N-1 electrons, respectively; $p_k(N+1)$and$p_k(N-1)$ denote atomic charge of atom k in molecular with N + 1 and N − 1 electrons, respectively. These

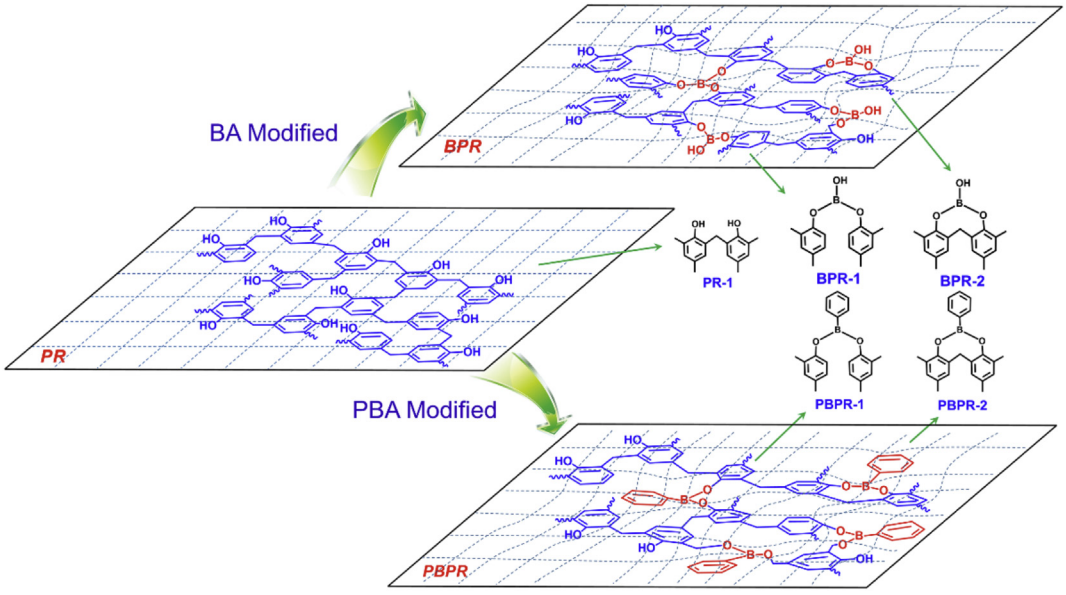

Fig. 1. Schematic represent of the boric acid and phenylboronic acid-modified PRs and their simplified models.

calculations were performed using G09, with the aid of Multiwfn software [29].

The BDE at both 0 K and 298 K were obtained. The BDE of chemical bond A-B in molecule AB defined as enthalpy change when the bond is cleaved (reaction 3) at certain temperature [30,31].

$$A - B \rightarrow A\bullet + B\bullet \quad (3)$$

$$\Delta H_T(A - B) = H_T(A\bullet) + H_T(B\bullet) - H_T(A - B) \quad (4)$$

$$BDE(0K) = \Delta H_{0K}(A - B) \quad (5)$$

$$BDE(298K) = \Delta H_{298K}(A - B) \quad (6)$$

Here, H denotes as the enthalpy of molecules or free radicals at certain temperature.

The homolytic products of each model were optimized with unrestricted open-shell method. Based on the molecular energy and vibrational frequencies obtained from G09, thermodynamic data (G and H) of the molecules or the free radicals (pyrolytic products) at 898 K were calculated by KiSTheIP [32] software. The scale factor used for frequency correction of BPW91/6-31G*, B3LYP/6-31G*, B3LYP-D3/6-31G*, CAM-B3LYP/def2-TZVP and M06-2X-D3/def2-TZVP were 0.986, 0.991, 0.991, 0.990 and 0.983, respectively [33]. Detailed steps to calculate the BDE, thermodynamic data and electronic structure data can be found in SI (Page 1–2).

3. Results and discussion

3.1. Bond strength

3.1.1. Weak bonds and corresponding analysis method

All chemical bonds in PR and boron-containing PRs could be ruptured at high temperature, but the stability of these bonds are different. Based on the handbook of BDEs [34,35], we can predict that C–C bond in methylene bridge, C–O/O–H bonds in the phenolic hydroxyl and C–O bond in borate structure are the weak bonds in the cured PR and boron-containing PRs, which will be cracked firstly. According to the damage extent caused by the homolytic reaction, the bonds in these models could be classified into skeleton rupturing bonds (Fig. 2, brown double arrow) and free radical producing bonds (Fig. 2, light blue single arrow). Such classification would facilitate the analysis of the influence of the homolytic reactions on the thermal stability of different bonds.

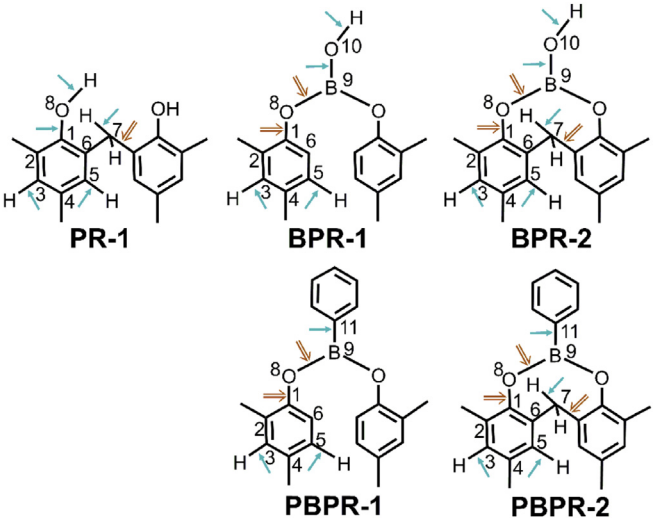

Fig. 2. Weak bonds in PR-1 and boron-containing PR models (⟹ skeleton rupturing bonds, ⟶ free radical producing bonds).

In general, BDE is a credible index to evaluate the strength of chemical bond, whereas sometimes it is difficult to be calculated for specific chemical bonds. For example, an optimization job towards the homolytic products of B–O(8), C–O(8) and C–C(7) in BPR-2 and PBPR-2 would be difficult to complete, since these bonds tend to rebuild during the geometry optimization. A precisely calculation of bond order will be helpful to evaluate the strength of these bonds [27,36]. Among the bond order calculation methods [37–39], the Mayer bond order was reliable to evaluate the bond strength [40]. Generally, for the same kind of bond in different chemical environment, a higher bond order reflects a higher bond strength [40,41]. Besides, an analysis of the geometry data of the above models will provide further information of bond strength and thermal stability [13].

3.1.2. BDE

The BDEs of main bonds in the five models at 298 K obtained from different methods were listed in Table 1 and compared with the reference value. The enthalpy of the five models and their homolytic products at 298 K, as well as BDEs at 0 K, can be found in (SITables 1 and 2). The accuracy of the five computational methods was evaluated mainly based on BDEs of bonds in PR-1 and reference values, as the referenced bonds for PR-1 share the most similar chemical environment with the bonds in PR-1.

Except for O(8)-H bond on CAM-B3LYP/def2-TZVP level and C–C(7) bond on M06-2X-D3/def2-TZVP level, the results on both the CAM-B3LYP/def2-TZVP and M06-2X-D3/def2-TZVP levels showed good accuracy for the most bonds. Poor results were obtained for C–C(7), C–O(8) and O(8)-H bonds on both the BPW91/6-31G* and B3LYP/6-31G* levels. The accuracy of BDEs of the C–C(7) and C–O(8) bonds was significantly enhanced with D3 correction on the B3LYP/6-31G* level. All the five methods showed good accuracy for BDEs of C–H bonds in the phenol rings. Owing to the good accuracy of BDEs calculated on CAM-B3LYP/def2-TZVP and M06-2X-D3/def2-TZVP levels, a comparison towards BDEs of bonds in different models was made mainly on these two levels.

On the CAM-B3LYP/def2-TZVP level, BDEs of both C–O and B–O bonds in C–O–B–O–C bridge (BPR-1 and PBPR-1) are higher than C–C in C–C–C bridges (PR-1), which is in agreement with the experimental deduction in the literature [5,6]. A further corollary could be inferred is that the C–O–B–O–C and C–C–C bridges in BPR-2 or PBPR-2 had equivalent strength compared to those in BPR-1 or PBPR-1. Unfortunately, optimization towards the homolytic products of B–O(8), C–O(8) and C–C(7) bonds in both BPR-2 and PBPR-2 failed, since all of these bonds were rebuilt after the homolytic products were optimized. In Section 3.1.3, bond order and geometry data were employed to further analyze the strength of these bonds.

Due to the influence of the neighboring borate structure, the BDEs of C–H in methylene bridge in BPR-2 and PBPR-2 were higher than that in PR-1, which indicated that much less H· radicals will be produced from the fracture of C–H bond in BPR-2 and PBPR-2. The BDEs of B–O(10) and O(10)-H in BPR-1 (and BPR-2) were higher than that of C–O(8) and O(8)-H in PR-1, respectively. Therefore, it can be speculated that the introduction of borate structure (BPR-1 and BPR-2) hindered the formation of free radicals (H· and HO·) at the initial stage of pyrolysis. The rupture of C–O(8), O(10)-H and C(11)-B bonds would lead to the formation of boron oxide, which may melt at ca. 450 °C and cover on the surface of unpyrolyzed regions to isolate the resin from being attacked by the free radicals [42,43].

It had been proved that PR or boron-containing PRs lost weight drastically at the range of 798–898 K, hence an analysis of the

Table 1
Calculated BDEs (kJ/mol, 298 K) of chemical bonds in PR-1 and boron-containing PR models and compared with reference value.

Models	Bonds	BPW91/6-31G*	B3LYP/6-31G*	B3LYP-D3/6-31G*	CAM-B3LYP/def2-TZVP	M06-2X-D3/def2-TZVP	*Ref. value*	*Ref. Bonds*
PR-1	C–C(7)	338.38	343.34	372.94	372.62	352.71	378.2 ± 8.4 (*T*)[a]	Ph–CH_2Ph
	C–O(8)	403.16	409.65	460.54	431.39	453.19	465.7 ± 4.2 (*T*)	Ph–OH
	O(8)-H	291.97	309.36	302.81	321.87	319.07	342.3 (*E*)[b]	PhO–H
	C(7)-H	324.34	329.13	333.87	334.19	339.99	353.5 ± 2.1 (*T*)	Ph_2CH–H
	C(3)-H	452.36	465.74	465.65	451.27	467.51	462.8 ± 14.2 (*E*)	PhOH(C3–H)[c]
	C(5)-H	451.55	464.68	467.70	449.69	467.86	462.8 ± 14.2 (*E*)	PhOH(C3–H)
BPR-1	C–O(8)	396.87	419.04	460.80	482.82	444.37	415.1 ± 5.9 (*E*)	Ph–OCH_3
	B–O(8)	403.56	424.81	462.38	471.32	439.04	481 ± 109 (*E*)	$(RO)_2$B–OCH_3
	B–O(10)	561.51	564.32	608.05	604.77	594.42	553 ± 30 (*E*)	$(HO)_2$B–OH
	O(10)-H	410.29	442.53	446.86	491.15	469.89	–	–
	C(3)-H	455.48	466.87	469.53	458.90	460.23	462.8 ± 14.2 (*E*)	PhOH(C3–H)
	C(5)-H	464.65	464.32	468.62	454.55	456.66	462.8 ± 14.2 (*E*)	PhOH(C3–H)
PBPR-1	C–O(8)	349.70	378.80	434.21	458.41	421.12	415.1 ± 5.9 (*E*)	Ph–OCH_3
	B–O(8)	392.00	404.04	463.03	478.63	438.53	481 ± 109 (*E*)	$(RO)_2$B–OCH_3
	C–B(11)	470.32	482.32	512.59	500.35	488.77	510 (*E*)	Cl_2B–Ph
	C(3)-H	451.08	464.67	465.58	464.61	464.59	462.8 ± 14.2 (*E*)	PhOH(C3–H)
	C(5)-H	452.87	465.58	466.16	466.05	466.45	462.8 ± 14.2 (E)	PhOH(C3–H)
BPR-2	B–O(10)	557.38	561.25	603.09	615.20	607.73	553 ± 30 (*E*)	$(HO)_2$B–OH
	O(10)-H	388.84	437.05	433.13	491.53	478.51	–	–
	C(7)-H	346.83	359.17	358.25	370.94	362.57	353.5 ± 2.1 (*T*)	Ph_2CH–H
	C(3)-H	450.65	464.62	465.81	465.46	466.96	462.8 ± 14.2 (*E*)	PhOH(C3–H)
	C(5)-H	452.59	466.13	466.46	465.92	467.79	462.8 ± 14.2 (*E*)	PhOH(C3–H)
PBPR-2	C–B(11)	465.07	479.93	502.13	490.40	480.45	510 (*E*)	Cl_2B–Ph
	C(7)-H	360.48	373.76	379.06	393.47	380.83	353.5 ± 2.1 (*T*)	Ph_2CH–H
	C(3)-H	452.33	464.90	466.58	466.12	466.33	462.8 ± 14.2 (*E*)	PhOH(C3–H)
	C(5)-H	450.61	465.87	466.07	465.74	465.58	462.8 ± 14.2 (*E*)	PhOH(C3–H)

[a] (*T*) denotes as Theoretical Value.
[b] (*E*) denotes as Experimental Value.
[c] PhOH(C3–H) denotes as C_3–H bond in PhOH.

ΔH_{898K} and ΔG_{898K} (SI Tables 3 and 4) of homolytic reaction of main bonds in these models would be helpful to understand the pyrolysis behavior in this temperature range. The ΔH_{898K} and ΔG_{898K} of B–O and O–H in boric hydroxyls, as well as C–H in phenol rings were higher than the other bonds. This suggested more heat was absorbed when these bonds were ruptured and less free radicals would be produced. Since the ΔG_{898K} of these bonds was considerably larger than 0, the homolytic reactions of these bonds were hard to sustain. That would be benefit to reduce the concentration of H· and HO· and slow down the rate of pyrolysis. However, the homolytic reactions of C–C(7), C–O(8) and O(8)-H in PR-1, as well as C–O(8) and B–O(8) in BPR-1 and PBPR-1 continued until all of them ruptured down, for both the ΔH_T and ΔG_T of these bonds were relatively lower than the others.

3.1.3. Bond order and geometry

Since the bond order of bonds in these models were obtained from different electronic structure, the absolute value of bond order in different models should not be compared directly. A referential bond with known BDE can be specified for comparison of the bond strength of the same bond in different models. For example, the C(7)-H could be considered as the referential bond to compare the strength of the C–C–C bridge in PR-1, BPR-2 and PBPR-2, for both the BDE and bond order of C(7)-H bond in the three models were very close to each other (Fig. 3). Similarly, B–O(10) could be considered as the referential bond to compare the strength of B–O(8) and C–O(8) bond in BPR-1 and BPR-2, while B–C could be considered as the referential bond to compare the strength of B–O(8) and C–O(8) bond in PBPR-1 and PBPR-2.

On both the M06-2X-D3/6-311G** and B3LYP-D3/6-311G** levels, the bond order of C–C bond in PR-1 was close to that in BPR-2 and PBPR-2, which indicated that the strength of C–C in methylene bridges in the PR-1, BPR-2 and PBPR-2 were equivalent to each other. Combined with the analysis of BDE of B–O(8) and C–O(8) in BPR-1 and PBPR-1 (Table 1), it can be said that the strength of C–O–B–O–C and C–C–C bridge in BPR-2 or PBPR-2 were fairly close, which would markedly improve the thermal stability of boron-containing PRs. Although quantitative results of the strength of O–B–O–C and C–C–C bridges were not obtained from the above analysis, we can verify the assumption that borate structure would affect the neighboring structures and consequently the thermal stability of the resin dramatically. The bond order on the B3LYP/6-31G* and BPW91/6-31G* levels show the same trend with the method mentioned above (SI Fig. 2).

The bond length of C–O in both BPR-1 and PBPR-1 were comparable to that in PR-1 (SI Table 5), which would be another evidence that the strength of C–O–B–O–C and C–C–C bridge in BPR-2 or PBPR-2 were fairly close. Calculations of the centroid distance and angle between the two phenol rings in each model showed that the distance between two phenol rings in PBPR-1 and PBPR-2 were closer than that in PR-1, BPR-1 and BPR-2 (Fig. 4, SI Table 6 and SI Table 7), which was beneficial to the char formation during the pyrolysis [42].

3.2. Reactivity of functional groups

Besides the BDE of main bonds in the resin, the reactivity of phenolic hydroxyl, boric hydroxyl, methylene, borate, phenylboronate and phenol ring was another important factor that affect the thermal stability of the resin. During the pyrolysis of PR resin, free radical substitution rules supreme after the homolytic reaction [1,2,14]. In the initial stage of free radical substitution reaction, the free radical were attracted by the electrostatic potential and the reactivity of the target functional groups could be evaluated by the net atomic charges [44]. Among the atomic charge calculation methods [45,46], the Mulliken charge, which was put forward in 1955 [47–49], was reliable to evaluate the electrostatic potential. However, when the distance between the radicals and target group was close enough, the electron cloud began to overlap and the electron population began to change significantly. Fukui function, instead of atomic charge would be more precise to present the reactivity of functional groups during this stage, as proposed by

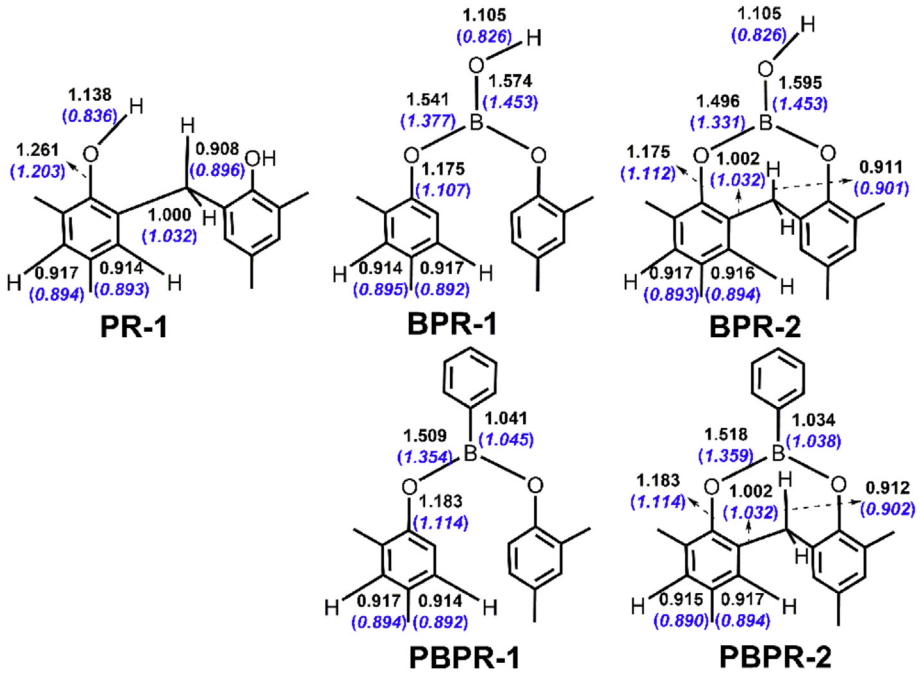

Fig. 3. Mayer bond orders of chemical bonds in PR-1 and boron-containing PR models (Normal and italic numbers represented as bond orders obtained on *M06-2X-D3/6-311G**** and *B3LYP-D3/6-311G**** levels, respectively).

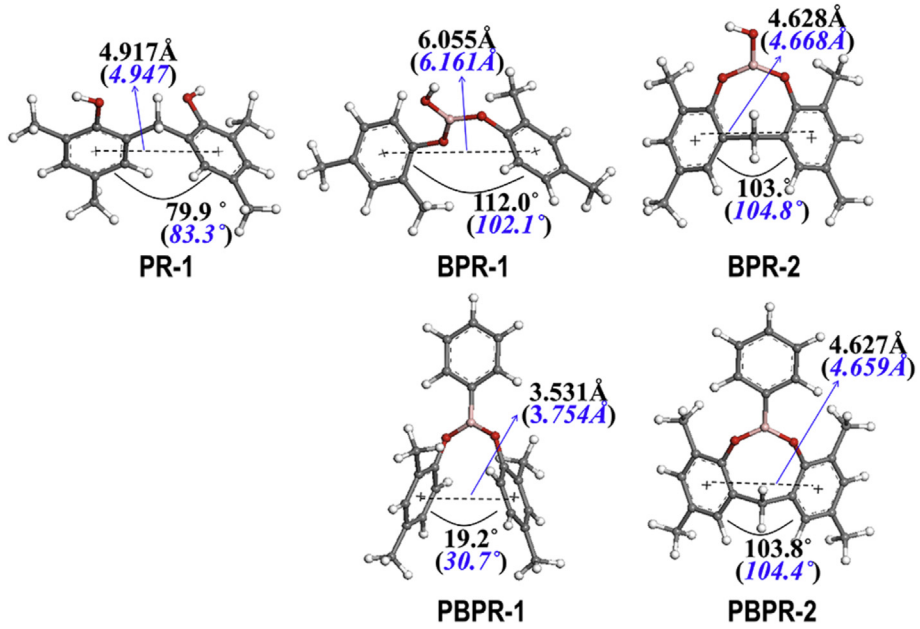

Fig. 4. The centroids distance and angle between the two phenol rings (Normal and italic numbers represented as data obtained by on *M06-2X-D3/def2-TZVP* and *B3LYP-D3/6-31G*** levels, respectively).

Paul et al. [28]. Further information of reactivity and thermal stability of these models could be obtained from HOMO distribution and energy level.

3.2.1. Mulliken charge

The atomic charges of oxygen atoms in boron-containing models was slightly negative than that in PR-1 (Fig. 5), which suggested that the borate structure would attract more radical than phenolic hydroxyl. In comparison with PR-1, negative charges on C atoms of methylene in BPR-2 and PBPR-2 were slightly increased, which may result in the increased reactivity of methylene. However, the charges on the two O atoms next to the C atom in methylene were more negative than the C atom itself, which reduced the possibility of being attacked by the radicals. A comprehensive comparison of net charge on O atom based on M06-2X-D3/6-311G** and B3LYP-D3/6-311G** methods showed that the reactivity of borate structure in boron-containing models was approximately equivalent to that of phenolic hydroxyl in PR-1. Population analysis based on the B3LYP/6-31G* and BPW91/6-31G* levels showed the similar results with the above method (SI Fig. 3). It

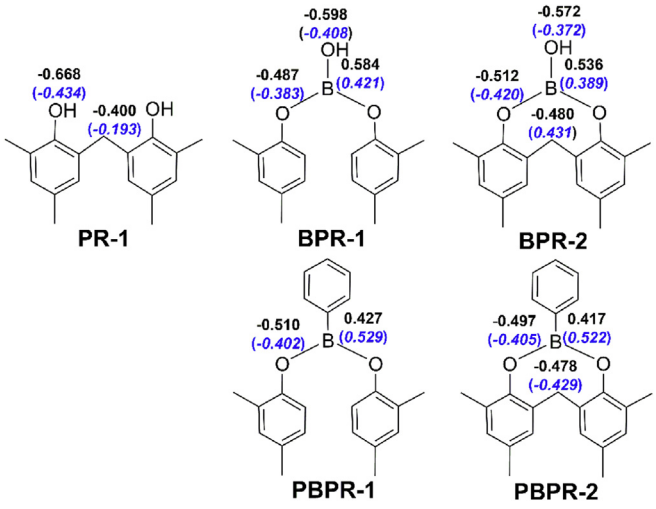

Fig. 5. Mulliken Charge of atoms in PR-1 and boron-containing models (Normal and italic numbers represented as Mulliken Charge obtained on *M06-2X-D3/6-311G*** and *B3LYP-D3/6-311G*** levels, respectively).

should be noted that boron oxide would be formed as a result of the radical attack of the borate structure, which will not induce further damage on the resin [42,43]. However, the hydroxyl radicals peeled from phenolic rings will lead to obvious destruction of the resin skeleton [14,50].

3.2.2. Fukui function

Fukui function for free radical attack ($f^0(r)$) of the above models were calculated on both the M06-2X-D3 and B3LYP-D3 methods. The isosurface (isovalue = 0.0028 a.u.) of $f^0(r)$ based on M06-2X-D3 (Fig. 6) indicated that phenolic hydroxyl, methylene and phenolic ring were the possible active cites, which may be attacked by the free radicals. Moreover, in comparison with PR-1, the distribution of $f^0(r)$ in boron-containing models was significantly changed. For example, the active zone of PBPR-1 and PBPR-2 was partially transferred to borate structure from phenolic ring, which meant that the incorporation of phenylboronate structure was beneficial to improve the thermal stability of PR. The isosurface of $f^0(r)$ based on B3LYP-D3 showed the identical distribution with M06-2X-D3 (SI Fig. 4).

Fukui indices ($f_k^0(r)$, condensed Fukui indices for free radical attack) for each atom in the above molecules were calculated based on the Hirshfeld charges (SI Table 8). Compared with PR-1, the $f_k^0(r)$ of C(1), C(2), C(4) and O(8) in PBPR-1 and PBPR-2 were significantly reduced, which was in accordance with the analysis result of $f^0(r)$ isosurface and Mulliken charge. Compared with BPR-1 and BPR-2, the $f_k^0(r)$ of B atom in PBPR-1 and PBPR-2 were increased, which meant that phenylboronate structure may attract more radicals and consequently both the phenol ring and methylene bridge will be protected.

3.2.3. HOMOs

The energy level of HOMOs of the five models based on all levels (SI Table 9) showed the same trend: BPR-1 < BPR-2 < PBPR-1 < PBPR-2 < PR-1, which means that the reactivity of all the boron-containing models are lower than PR-1. This was consistent with the study conducted by Wu et al. [13], since they also approved that HOMO distribution of benzene-containing structure will be significantly changed due to the incorporation of boron atom.

A Comparison of HOMO distribution between the five models (Fig. 7) showed that the phenolic hydroxyl, borate structure and phenol ring are the active sites, which indicates that C–O–B–O–C bridge would also suffer from damage inevitably. However, it is worth to point out that there is HOMO distributed on methylene in PR-1, whereas no HOMO distributes on methylenes in BPR-2 and PBPR-2. A conclusion could be inferred from above analysis that the incorporation of C–O–B–O–C bridge into PR would be beneficial to improve the thermal stability of PR skeleton.

4. Conclusion

Based on simplified models of PR, BPR and PBPR, the BDEs of main bonds and the reactivity of main functional groups were obtained with BPW91, B3LYP, CAM-B3LYP and M06-2X methods.

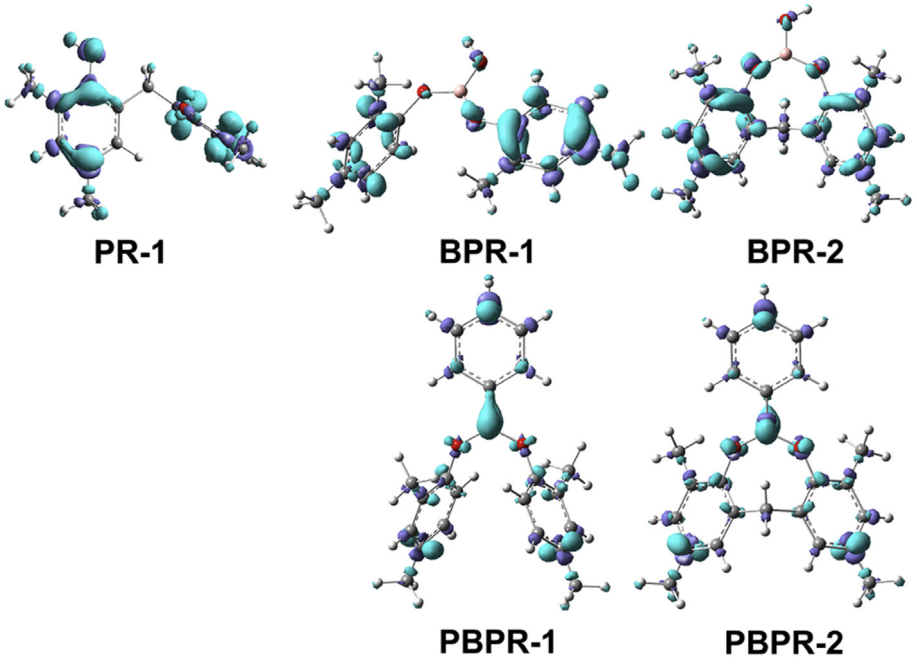

Fig. 6. Isosurface of Fukui function for radical attack of PR-1 and boron-containing models. (Isovalue = 0.0028 a.u., *M06-2X-D3/6-311G***).

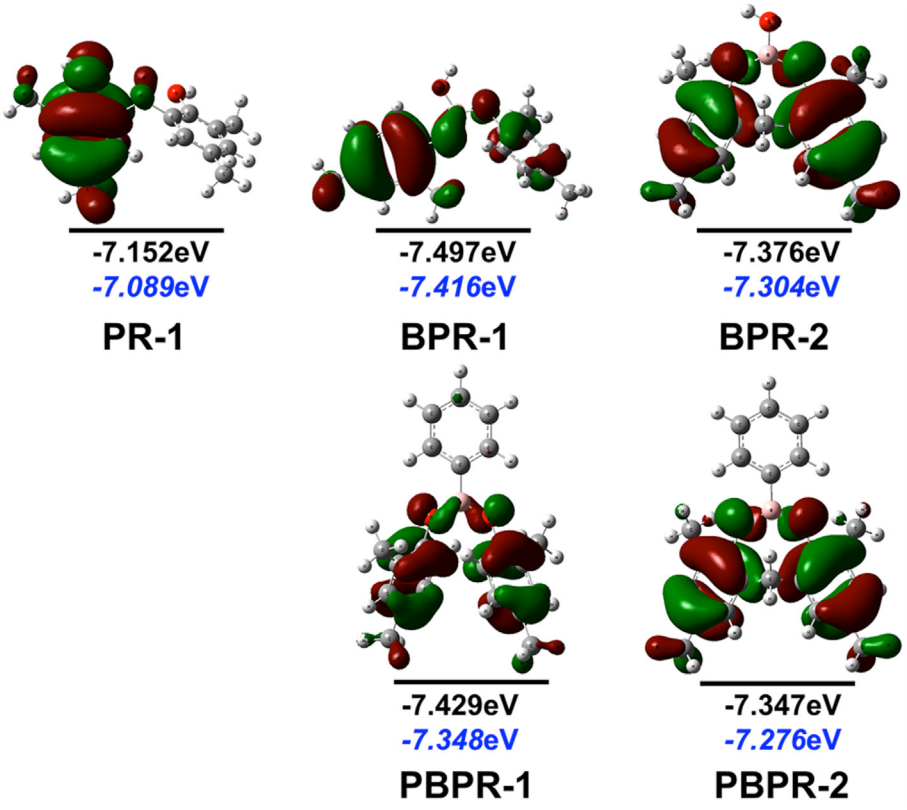

Fig. 7. HOMOs of PR-1 and boron-containing models (Isovalue = 0.02 a.u., Normal and italic numbers represented as HOMO energy levels obtained on *M06-2X-D3/6-311G*** and *B3LYP-D3/6-311G*** levels, respectively).

The introduction of borate structure could improve the thermal stability of PR significantly, which can be attributed to the high BDE of B–O bond and the changed reactivity of boron-neighboring structure in the cured resin. The phenolic hydroxyl, methylene, boric hydroxyl and phenol ring showed higher reactivity than that of borate and phenylboronates. In the models with eight-membered ring formed by C–O–B–O–C bridge and C–C–C bridge, the reactivity of methylene was significantly reduced, which was beneficial to the thermal stability of boron-containing PRs. Our theoretical approach has provided a reasonable explanation of the experimental results that boric acid and phenylboronic acid could improve the thermal stability of PR substantially.

Acknowledgment

The authors would like to acknowledge the financial support to this work provided by the National Natural Science Foundation of China through grant No. 51273160 and No. 51473134.

Appendix A. Supplementary data

Supplementary data related to this article can be found at http://dx.doi.org/10.1016/j.polymdegradstab.2015.05.009.

References

[1] K.A. Trick, T.E. Saliba, Mechanisms of the pyrolysis of phenolic resin in a carbon/phenolic composite, Carbon 33 (1995) 1509–1515, http://dx.doi.org/10.1016/0008-6223(95)00092-R.
[2] Y. Chen, Z. Chen, S. Xiao, H. Liu, A novel thermal degradation mechanism of phenol–formaldehyde type resins, Thermochim Acta 476 (2008) 39–43, http://dx.doi.org/10.1016/j.tca.2008.04.013.
[3] W.M. Jackson, R.T. Conley, High temperature oxidative degradation of phenol–formaldehyde polycondensates, J Appl Polym Sci 8 (1964) 2163–2193, http://dx.doi.org/10.1002/app.1964.070080516.
[4] M. Blazso, T. Toth, Thermal decomposition of methylene bridges and methyl groups at aromatic rings in phenol-formaldehyde polycondensates, J Anal Appl Pyrolysis 10 (1986) 41–50, http://dx.doi.org/10.1016/0165-2370(86)85018-5.
[5] J. Gao, Y. Liu, F. Wang, Structure and properties of boron-containing bisphenol-A formaldehyde resin, Eur Polym J 37 (2001) 207–210, http://dx.doi.org/10.1016/S0014-3057(00)00095-1.
[6] M.O. Abdalla, A. Ludwick, T. Mitchell, Boron-modified phenolic resins for high performance applications, Polymer 44 (2003) 7353–7359, http://dx.doi.org/10.1016/j.polymer.2003.09.019.
[7] Y. Liu, X. Jing, Pyrolysis and structure of hyperbranched polyborate modified phenolic resins, Carbon 45 (2007) 1965–1971, http://dx.doi.org/10.1016/j.carbon.2007.06.008.
[8] S. Wang, X. Jing, Y. Wang, J. Si, High char yield of aryl boron-containing phenolic resins: the effect of phenylboronic acid on the thermal stability and carbonization of phenolic resins, Polym Degrad Stab 99 (2014) 1–11, http://dx.doi.org/10.1016/j.polymdegradstab.2013.12.011.
[9] A.H. Conner, Predicting the reactivity of phenolic compounds with formaldehyde under basic conditions: an ab initio study, J Appl Polym Sci 78 (2000) 355–363, http://dx.doi.org/10.1002/1097-4628(20001010)78, 2<355::AID-APP150>3.0.CO;2–3.
[10] T. Mitsunaga, A.H. Conner, C.G. Hill, Predicting the reactivity of phenolic compounds with formaldehyde. II. Continuation of an ab initio study, J Appl Polym Sci 86 (2002) 135–140, http://dx.doi.org/10.1002/app.10926.
[11] V.D. Khavryuchenko, O.V. Khavryuchenko, Quantum chemical simulation of phenol-formaldehyde resin carbonization in the presence of phosphoric acid: computational evidence of Michaelis–Arbuzov-type reaction, J Phys Chem C 117 (2013) 7628–7635, http://dx.doi.org/10.1021/jp4000736.
[12] G. Frison, G. Ohanessian, A comparative study of semiempirical, ab initio, and DFT methods in evaluating metal–ligand bond strength, proton affinity, and interactions between first and second shell ligands in Zn-biomimetic complexes, J Comput Chem 29 (2008) 416–433, http://dx.doi.org/10.1002/jcc.20800.
[13] X. Wu, L.R. Radovic, Ab initio molecular orbital study on the electronic structures and reactivity of boron-substituted carbon, J Phys Chem A 108 (2004) 9180–9187, http://dx.doi.org/10.1021/jp048212w.
[14] T. Qi, C.W. Bauschlicher Jr., J.W. Lawson, T.G. Desai, E.J. Reed, Comparison of ReaxFF, DFTB, and DFT for phenolic pyrolysis. 1. Molecular dynamics simulations, J Phys Chem A 117 (2013) 11115–11125, http://dx.doi.org/10.1021/

jp4081096.
[15] A.D. Becke, Density-functional exchange-energy approximation with correct asymptotic behavior, Phys Rev A 38 (1988) 3098, http://dx.doi.org/10.1103/PhysRevA.38.3098.
[16] C. Lee, W. Yang, R.G. Parr, Development of the Colle-Salvetti correlation-energy formula into a functional of the electron density, Phys Rev B 37 (1988) 785–789, http://dx.doi.org/10.1103/PhysRevB.37.785.
[17] J.P. Perdew, J. Chevary, S. Vosko, K.A. Jackson, M.R. Pederson, D. Singh, et al., Atoms, molecules, solids, and surfaces: applications of the generalized gradient approximation for exchange and correlation, Phys Rev B 46 (1992) 6671, http://dx.doi.org/10.1103/PhysRevB.46.6671.
[18] P. Stephens, F. Devlin, C. Chabalowski, M.J. Frisch, Ab initio calculation of vibrational absorption and circular dichroism spectra using density functional force fields, J Phys Chem 98 (1994) 11623–11627, http://dx.doi.org/10.1021/j100096a001.
[19] T. Yanai, D.P. Tew, N.C. Handy, A new hybrid exchange–correlation functional using the Coulomb-attenuating method (CAM-B3LYP), Chem Phys Lett 393 (2004) 51–57, http://dx.doi.org/10.1016/j.cplett.2004.06.011.
[20] F. Weigend, R. Ahlrichs, Balanced basis sets of split valence, triple zeta valence and quadruple zeta valence quality for H to Rn: design and assessment of accuracy, Phys Chem Chem Phys 7 (2005) 3297–3305, http://dx.doi.org/10.1039/B508541A.
[21] Y. Zhao, D.G. Truhlar, The M06 suite of density functionals for main group thermochemistry, thermochemical kinetics, noncovalent interactions, excited states, and transition elements: two new functionals and systematic testing of four M06-class functionals and 12 other functionals, Theor Chem Acc 120 (2008) 215–241, http://dx.doi.org/10.1007/s00214-007-0310-x.
[22] S. Grimme, J. Antony, S. Ehrlich, H. Krieg, A consistent and accurate ab initio parametrization of density functional dispersion correction (DFT-D) for the 94 elements H-Pu, J Chem Phys 132 (2010) 154104, http://dx.doi.org/10.1063/1.3382344.
[23] K. Theilacker, A.V. Arbuznikov, H. Bahmann, M. Kaupp, Evaluation of a combination of local hybrid functionals with DFT-D3 corrections for the calculation of thermochemical and kinetic data, J Phys Chem A 115 (2011) 8990–8996, http://dx.doi.org/10.1021/jp202770c.
[24] J. Zheng, X. Xu, D. Truhlar, Minimally augmented Karlsruhe basis sets, Theor Chem Acc 128 (2011) 295–305, http://dx.doi.org/10.1007/s00214-010-0846-z.
[25] A. Baishya, V. Mundlapati, S. Nembenna, H. Biswal, Structure, bonding and energetics of N-heterocyclic carbene (NHC) stabilized low oxidation state group 2 (Be, Mg, Ca, Sr and Ba) metal complexes: a theoretical study, J Chem Sci 126 (2014) 1781–1788, http://dx.doi.org/10.1007/s12039-014-0657-1.
[26] M.J. Frisch, G.W. T, H.B. Schlegel, G.E. Scuseria, M.A. Robb, J.R. Cheeseman, et al., Gaussian 09, revision A. 02, Gaussian. Inc, Wallingford, CT, 2009.
[27] I. Mayer, Bond orders and valences from ab initio wave functions, Int J Quantum Chem 29 (1986) 477–483, http://dx.doi.org/10.1002/qua.560290320.
[28] P.W. Ayers, R.G. Parr, Variational principles for describing chemical reactions: the Fukui function and chemical hardness revisited, J Am Chem Soc 122 (2000) 2010–2018, http://dx.doi.org/10.1021/ja9924039.
[29] T. Lu, F. Chen, Multiwfn: a multifunctional wavefunction analyzer, J Comput Chem 33 (2012) 580–592, http://dx.doi.org/10.1002/jcc.22885.
[30] S.J. Blanksby, G.B. Ellison, Bond dissociation energies of organic molecules, Acc Chem Res 36 (2003) 255–263, http://dx.doi.org/10.1021/ar020230d.
[31] T. Vreven, K. Morokuma, The accurate calculation and prediction of the bond dissociation energies in a series of hydrocarbons using the IMOMO (integrated molecular orbital+ molecular orbital) methods, J Chem Phys 111 (1999) 8799–8803, http://dx.doi.org/10.1063/1.480227.
[32] S. Canneaux, F. Bohr, E. Henon, KiSThelP: a program to predict thermodynamic properties and rate constants from quantum chemistry results†, J Comput Chem 35 (2014) 82–93, http://dx.doi.org/10.1002/jcc.23470.
[33] I. Alecu, J. Zheng, Y. Zhao, D.G. Truhlar, Computational thermochemistry: scale factor databases and scale factors for vibrational frequencies obtained from electronic model chemistries, J Chem Theory Comput 6 (2010) 2872–2887, http://dx.doi.org/10.1021/ct100326h.
[34] Y.-R. Luo, Handbook of bond dissociation energies in organic compounds, CRC Press, 2002.
[35] Y.-R. Luo, Comprehensive handbook of chemical bond energies, CRC Press, 2007.
[36] A.J. Bridgeman, G. Cavigliasso, L.R. Ireland, J. Rothery, The Mayer bond order as a tool in inorganic chemistry, J Chem Soc Dalton Trans (2001) 2095–2108, http://dx.doi.org/10.1039/B102094N.
[37] K.B. Wiberg, Application of the pople-santry-segal CNDO method to the cyclopropylcarbinyl and cyclobutyl cation and to bicyclobutane, Tetrahedron 24 (1968) 1083–1096, http://dx.doi.org/10.1016/0040-4020(68)88057-3.
[38] I. Mayer, Charge, bond order and valence in the ab initio SCF theory, Chem Phys Lett 97 (1983) 270–274, http://dx.doi.org/10.1016/0009-2614(83)80005-0.
[39] J. Cioslowski, S.T. Mixon, Covalent bond orders in the topological theory of atoms in molecules, J Am Chem Soc 113 (1991) 4142–4145, http://dx.doi.org/10.1021/ja00011a014.
[40] T. Lu, F. Chen, Bond order analysis based on the Laplacian of electron density in fuzzy overlap space, J Phys Chem A 117 (2013) 3100–3108, http://dx.doi.org/10.1021/jp4010345.
[41] A.J. Bridgeman, G. Cavigliasso, Towards an understanding of the bonding in polyoxometalates through bond order and bond energy analysis, Faraday Discuss 124 (2003) 239–258, http://dx.doi.org/10.1039/B210795N.
[42] C. Martin, J. Ronda, V. Cadiz, Development of novel flame-retardant thermosets based on boron-modified phenol–formaldehyde resins, J Polym Sci Part A: Polym Chem 44 (2006) 3503–3512, http://dx.doi.org/10.1002/pola.21458.
[43] S. Wang, X. Jing, Y. Wang, J. Si, Synthesis and characterization of novel phenolic resins containing aryl-boron backbone and their utilization in polymeric composites with improved thermal and mechanical properties, Polym Adv Technol 25 (2014) 152–159, http://dx.doi.org/10.1002/pat.3216.
[44] S. Cox, D. Williams, Representation of the molecular electrostatic potential by a net atomic charge model, J Comput Chem 2 (1981) 304–323, http://dx.doi.org/10.1002/jcc.540020312.
[45] A.E. Clark, J.L. Sonnenberg, P.J. Hay, R.L. Martin, Density and wave function analysis of actinide complexes: what can fuzzy atom, atoms-in-molecules, Mulliken, Löwdin, and natural population analysis tell us? J Chem Phys 121 (2004) 2563–2570, http://dx.doi.org/10.1063/1.1766292.
[46] S.M. Bachrach, Population analysis and electron densities from quantum mechanics, Rev Comput Chem 5 (2007) 171–228, http://dx.doi.org/10.1002/9780470125823.ch3.
[47] R.S. Mulliken, Electronic population analysis on LCAO-MO molecular wave functions .1, J Chem Phys 23 (1955) 1833–1840, http://dx.doi.org/10.1063/1.1740588.
[48] R.S. Mulliken, Electronic population analysis on LCAO-MO molecular wave functions. 2. Overlap populations, bond orders, and covalent bond energies, J Chem Phys 23 (1955) 1841–1846, http://dx.doi.org/10.1063/1.1740589.
[49] R.S. Mulliken, Electronic population analysis on LCAO-MO molecular wave functions. 3. Effects of hybridization on overlap and gross AO populations, J Chem Phys 23 (1955) 2338–2342, http://dx.doi.org/10.1063/1.1741876.
[50] D-e Jiang, A.C. Van Duin, W.A. Goddard III, S. Dai, Simulating the initial stage of phenolic resin carbonization via the ReaxFF reactive force field, J Phys Chem A 113 (2009) 6891–6894, http://dx.doi.org/10.1021/jp902986u.